http://eprints.gla.ac.uk/69391/

Deposited on: 28 September 2012

How feedback inhibition shapes spike-timing-dependent plasticity and its implications for recent Schizophrenia models

Bernd Porr[a], Lynsey McCabe[a], Paolo di Prodi[a], Christoph Kolodziejski[b,c,d], Florentin Wörgötter[b,c,d]

[a] School of Engineering, University of Glasgow, United Kingdom, G12 8QQ
[b] Bernstein Center for Computational Neuroscience, Göttingen, Germany
[c] Department for Computational Neuroscience, III. Physikalisches Institut - Biophysik, Georg-August-University Göttingen, Germany
[d] Network Dynamics Group, Max-Planck-Institute for Dynamics and Selforganization, Göttingen, Germany

Abstract

It has been shown that plasticity is not a fixed property but, in fact, changes depending on the location of the synapse on the neuron and/or changes of biophysical parameters. Here we investigate how plasticity is shaped by feedback inhibition in a cortical microcircuit. We use a differential Hebbian learning rule to model spike-timing dependent plasticity and show analytically that the feedback inhibition shortens the time window for LTD during spike-timing dependent plasticity but not for LTP. We then use a realistic GENESIS model to test two hypothesis about interneuron hypofunction and conclude that a reduction in GAD67 is the most likely candidate as the cause for hypofrontality as observed in Schizophrenia.

Keywords: Schizophrenia, GABA, NMDA, GAD67, STDP, Hebb, inhibition, PCP

1. Introduction

Spike-timing dependent plasticity (Markram et al., 1997; Magee and Johnston, 1997; Bi and Poo, 1998) is a special form of Hebbian learning (Hebb, 1949) where the order of the pre- and postsynaptic events determine weight growth or decay. Plotting different timings between pre- and postsynaptic potentials against the weight change leads to the so-called STDP curve. Typically pre- and then postsynaptic stimulation causes long term potentiation (LTP) while post- and then presynaptic stimulation causes long term depression (LTD). It has been shown that the STDP curve is not constant but changes its shape when the pre- and postsynaptic potentials change (Porr et al., 2004; Tamosiunaite et al., 2006; Voegtlin, 2009; Clopath et al., 2010). For example, backpropagating spikes can change the shape of the STDP curve and distal dendrites have their own STDP curves because the dynamics of the postsynaptic potentials is much slower far away from the soma (Tamosiunaite et al., 2007a). In contrast to the previous work we investigate here how external influences can change the STDP curve. In particular we investigate how feedback inhibition in a cortical microcircuit influences spike-timing dependent plasticity.

There is an abundance of different inhibitory neurons in the cortex which have specific roles and targets (Somogyi and Klausberger, 2005). Of special interest here are parvalbumine positive (PV+) perisomatic inhibitory interneurons which innervate the somata of pyramidal neurons and therefore have a direct influence on the membrane potential of the pyramidal neurons (Freund and Katona, 2007). These cells provide fast feedback inhibition as a prominent feature of cortical processing. Pyramidal neurons excite these inhibitory cells which in turn inhibit the pyramidal neurons. The inhibition has a strong effect on the postsynaptic dynamics of the pyramidal neuron by resetting the membrane potential quickly to the resting potential (Ulrich, 2003) which is known as shunting inhibition. As stated in the first paragraph, the shape of the postsynaptic potential will determine the shape of the STDP curve. Consequently, the shape of the STDP curve will be altered in the presence of the interneuron and by the timing and strength of the feedback.

Schizophrenia is a mental illness which affects about 1% of the population and has detrimental consequences for the patients. Popular hypotheses about the cause of Schizophrenia propose a hypofunction of the inhibitory system in the prefrontal cortex which later causes a hypofunction of the prefrontal activity. However, having less inhibition in the cortex would cause actually *more* activity in the cortex. We provide an explanation which predicts that less inhibition causes more LTD and therefore an overall slow decay of synaptic weights. We show that the part of the STDP curve which represents LTD is shorter in the presence of feedback inhibition. This result is a possible explanation for the observed depression in the prefrontal cortex after chronic application of the NMDA receptor antagonists which is a recent model for schizophrenia (Morris et al., 2005). Our model predicts that chronic Phencyclidine (PCP) treatment widens the time window for LTD and consequently causes more LTD in the cortical micro-circuitry. Thus, we provide an explanation why paradoxically less inhibition in the cortex leads eventually to less cortical activity (Andreasen et al., 1997; Ragland et al., 2007).

There are two main hypotheses which link reduced interneu-

Email addresses: `bernd.porr@gla.ac.uk` (Bernd Porr), `epokh@elec.gla.ac.uk` (Paolo di Prodi), `kolo@bccn-goettingen.de` (Christoph Kolodziejski), `worgott@physik3.gwdg.de` (Florentin Wörgötter)

ron activity to schizophrenia: one states that NMDA hypofunction in cortical interneurons is responsible for less interneuron activity (Morris et al., 2005) and the other states that there is less GABA released from the interneuron through a hypofunction of the GABA synthesizing enzyme GAD67 (Guidotti et al., 2005). In order to find out which of these hypotheses is more likely to be the cause of schizophrenia we have simulated both cases in realistic GENESIS simulations involving one pyramidal and one perisomatic inhibitory neuron. We will show that the GAD67 hypothesis is the clear winner.
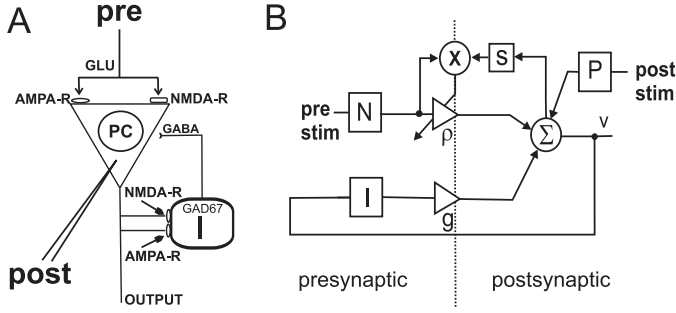

Figure 1: Model of the cortical microcircuit with a pyramidal cell (PC) and an interneuron (I). (A) "pre" is the excitatory input, a modelled presynaptic input into the pyramidal cell. Attached to the pyramidal cell are AMPA and NMDA receptors. "post" represents the current injection into the pyramidal cell stimulating the neuron inducing a postsynaptic action potential. (B) The analytical model. The symbol $\sum$ represents a summation node and $\otimes$ multiplication. N is the presynaptic input, the transfer function of the NMDA channel and P being the postsynaptic input, the transfer function of the postsynaptic potential. I is the feedback inhibition, which can be compared to the inhibitory interneuron I seen in (A), ρ the synaptic weight of the excitatory input, g the synaptic weight of the inhibitory input, and s is the derivative of the postsynaptic potential in the Laplace domain.

2. Materials and Methods

First we will explain the neurophysiological circuit and then we will extract the relevant properties from it so that we are able to treat the circuit analytically. Later we will go back to the original circuit in our GENESIS model. Fig. 1A depicts a typical microcircuit which consists of a pyramidal cell and an interneuron. Attached to the pyramidal cell are AMPA and NMDA receptors which have specific functions in our model: while the AMPA receptor represents the weight ρ which determines the amount of postsynaptic depolarisation, the NMDA receptor is responsible for the change in synaptic weight and therefore for a change in the number of AMPA receptors inserted into the membrane. Basically the AMPA weight change is proportional to the NMDA activation and the *change* (Yang et al., 1999; Lindskog et al., 2006) of the postsynaptic calcium concentration.

$$\frac{d\rho}{dt} = \mu \cdot \text{pre} \cdot \frac{d}{dt}\text{post} \tag{1}$$

where μ is the learning rate. This learning rule falls into the category of differential Hebbian learning rules (Klopf, 1986; Porr and Wörgötter, 2003) and models the STDP behaviour by

employing a derivative which allows analytical treatment while preserving the desired weight change, namely that the timing of the post- and pre-synaptic events determine if the synapse undergoes LTP or LTD.

A precise definition of the weight change will be made in the sections below. A current injection into the pyramidal cell stimulates the neuron enough to generate the postsynaptic action potential. This propagates from the pyramidal cell body down through the axon, causes glutamate release thereby activating the NMDA receptors on the GABAergic interneuron, allowing an influx of calcium into the cell. If the excitation is strong enough the interneuron releases GABAergic neurotransmitters back to the pyramidal cell, inhibiting as it does so. This inhibition is usually a shunting inhibition where the interneuron resets the pyramidal cell to resting potential. Note the difference between the pyramidal neuron and the interneuron: while the EPSP (excitatory postsynaptic potential) is generated by the AMPA receptors in case of the pyramidal neuron, the EPSP in the interneuron is generated by both the NMDA and AMPA receptors. We will discuss the implications of this later on when we compare the timings of NMDA and AMPA receptors and their actual contributions to the action potentials.

2.1. Analytical derivation of STDP with Feedback Inhibition

Fig. 1B shows the formalised circuit diagram of the cortical microcircuit. In order to achieve an analytical result we need to switch to the Laplace domain which allows a simple treatment of the feedback loop. Functions in the Laplace domain have capital letters and functions in the time domain have small letters. The feedback is modelled by the transfer function $I(s)$, the presynaptic activation by $N(s)$ (for NMDA) and the postsynaptic activation by $P(s)$ (for postsynaptic). The temporal derivative in the Laplace domain becomes a multiplication with s.

The presynaptic potential is represented by the standard NMDA channel model introduced by Koch (1998a):

$$n(t) \quad = \quad -\frac{1}{\frac{1}{\tau_{N1}} - \frac{1}{\tau_{N2}}}(e^{-\frac{t}{\tau_{N1}}} - e^{-\frac{t}{\tau_{N2}}}) \tag{2}$$

$$N(s) \quad = \quad \frac{1}{(s + \frac{1}{\tau_{N1}})(s + \frac{1}{\tau_{N2}})} \tag{3}$$

where τ_{N1} and τ_{N2} are rise- and decay-constants of the NMDA channel. Note that we have omitted here the magnesium block to be able to derive an analytical solution. For a more detailed justification of this omission we refer the reader to Porr et al. (2004).

The postsynaptic potential is modelled in the same way where we have τ_{P1} and τ_{P2} for the rise and fall times:

$$p(t) \quad = \quad -\frac{1}{\frac{1}{\tau_{P1}} - \frac{1}{\tau_{P2}}}(e^{-\frac{t}{\tau_{P1}}} - e^{-\frac{t}{\tau_{P2}}}) \tag{4}$$

$$P(s) \quad = \quad \frac{1}{(s + \frac{1}{\tau_{P1}})(s + \frac{1}{\tau_{P2}})} \tag{5}$$

which can be interpreted as the calcium concentration. Thus, the function $P(s)$ models the calcium response to a postsynaptic stimulation.

2

The feedback inhibition performed via the interneuron is modelled as a first order system to minimise the complexity of the solution and because the interneurons react virtually instantly (Zaitsev et al., 2007). Of central interest is here the decay of their inhibition because this is controlled by the internal calcium buffer parvalbumin (PV). The transfer function of the feedback inhibition is as follows:

$$i(t) = ge^{-\tau_I t} \Leftrightarrow I(s) = \frac{g}{s + \tau_I} \qquad (6)$$

where g is the gain of the feedback loop and τ_I the decay constant.

The total membrane potential is calculated in the following way:

$$V(s) = \rho N(s) + P(s) - I(s)V(s) \qquad (7)$$

where the function $P(s)$ models the postsynaptic response, the function $N(s)$ is the dynamic of the NMDA channel and $I(s)$ the transfer function of the inhibitory neuron, hence the negative sign used.

Spike-timing dependent plasticity is modelled by the product of the NMDA conductance $N(s)$ with the derivative of the postsynaptic potential which, for the analytical model, is just the membrane potential. Later in the GENESIS simulations we will replace it by the calcium concentration. The correlation in the time and Laplace domain is expressed as:

$$\Delta\rho(T) = \mu \int_0^{\infty} n(t)\frac{d}{dt}v(t-T)dt \qquad (8)$$
$$= \mu \int_{-\infty}^{\infty} N(-s)e^{-sT}V(s)ds \qquad (9)$$

which is called Plancherel's theorem (see Porr et al. (2004) for more details). Note that the presynaptic event always happens at $t = 0$ and the postsynaptic event is shifted by T.

Having all equations in the Laplace domain allows us to solve the feedback system analytically. Consequently, we can also calculate the STDP curve analytically (Porr et al., 2004).

We will show now analytically that inhibitory feedback influences the STDP curve in a very specific way, namely that it changes the *shape* of the negative part of the STDP curve ($T < 0$) while the positive part ($T > 0$) is scaled, only.

We can now solve Eq. 7 for the membrane potential $V(s)$:

$$V(s) = \frac{\rho N(s) + P(s)}{1 + I(s)} \qquad (10)$$

Substituting Eqs. 6 and 10 into Eq. 9 yields an integral which can be solved with the method of residuals. For $T > 0$ the solution is:

$$\Delta\rho(T) = \frac{\tau_{N2}(\tau_{N2}+\tau_I)e^{-\tau_{N2}T}}{(\tau_{N1}-\tau_{N2})(\tau_{N2}+\tau_{P1})(\tau_{N2}+\tau_{P2})(\tau_{N2}+\tau_I+g)}$$
$$- \frac{\tau_{N1}(\tau_{N1}+\tau_I)e^{-\tau_{N1}T}}{(\tau_{N1}-\tau_{N2})(\tau_{N1}+\tau_{P1})(\tau_{N1}+\tau_{P2})(\tau_{N1}+\tau_I+g)} \qquad (11)$$

where we see that the timing of the STDP curve is determined by the NMDA channel dynamics (rise and decay times, τ_{N1} and τ_{N2}).

For $T < 0$ the solution looks similar but with the difference that this part of the curve is determined by the postsynaptic dynamics (rise and decay times, τ_{P1} and τ_{P2}):

$$\Delta\rho(T) = \frac{\tau_{P1}(\tau_{P1}-\tau_I)e^{\tau_{P1}T}}{(\tau_{N1}+\tau_{P1})(\tau_{N2}+\tau_{P1})(\tau_{P1}-\tau_{P2})(\tau_{N1}-\tau_I-g)}$$
$$- \frac{\tau_{P2}(\tau_{P2}-\tau_I)e^{\tau_{P2}T}}{(\tau_{N1}+\tau_{P2})(\tau_{N2}+\tau_{P2})(\tau_{P1}-\tau_{P2})(\tau_{N2}-\tau_I-g)}$$
$$+ \frac{g(\tau_I+g)e^{(\tau_I+g)T}}{(\tau_{N1}+\tau_I+g)(\tau_{N2}+\tau_I+g)(\tau_{P1}-\tau_I-g)(\tau_{P2}-\tau_I-g)} \qquad (12)$$

The third term of Eq. 12 arises from the inhibitory feedback. This term becomes strong against the other two terms if either the gain g is high or if the time constant of the feedback is similar to one of the time constants of the postsynaptic potential.
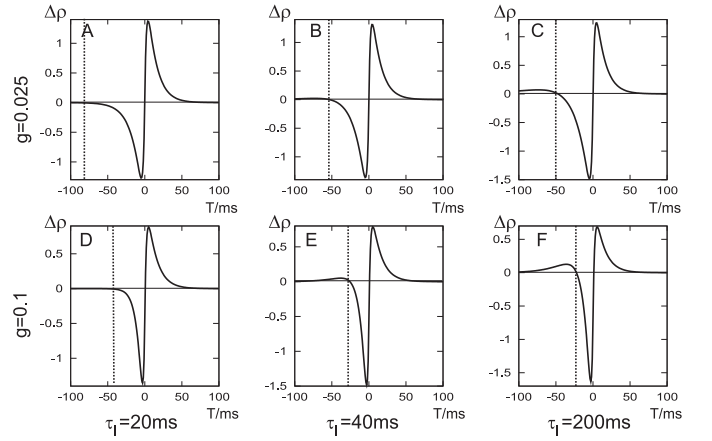

Figure 2: Spike-timing dependent plasticity curves with altered inhibition. The first row (A-C) shows STDP curves for $g = 0.025$ and the second one (D-F) STDP curves for $g = 0.1$. The decay time of the inhibition has been altered from left to right from $\tau_I = 20ms$ to $\tau_I = 200ms$. The dotted lines indicate the beginning of the LTD time window. Other parameters: $\tau_{N1} = 2.1ms$, $\tau_{N2} = 12.1ms$, $\tau_{P1} = 2.1ms$, $\tau_{P2} = 20.1ms$.

Fig. 2 shows the results for changing feedback where we have altered both the feedback gain g and the time constant τ_I of the feedback pathway. It can be seen that both parameters, gain and the time constant τ_I, influence the shape of the STDP curve. However, the inhibition only changes the *shape* of the negative part of the STDP curve while the positive part is scaled, only. We have added a line ($\Delta\rho < 0.01$) showing the beginning of the LTD time window coming from negative times.

It is clearly visible that the higher the gain of the feedback the shorter is the time window where the pyramidal neuron undergoes LTD. An increase of the gain from $g = 0.025$ to $g = 0.1$ in the first column ($\tau_I = 20ms$) reduces the time window from $80ms$ to $40ms$. Similar effects can be observed for longer values of the inhibitory decay rates τ_I. As mentioned earlier a change in the gain of the feedback loop can be caused by NMDA hypofunction in the interneuron, for example during PCP treatment. This means that less inhibition causes longer LTD time windows.

Also the decay rate of the inhibitory PSP τ_I influences the negative time window of the STDP curve. This can be seen in Fig. 2 within one row (A-C or D-F). Here, a longer decay (C,F) causes less LTD and a shorter decay more LTD (A,D).

3

The shortening of the LTD window is caused by a period of LTP for negative times $T < 0$ (post $\rightarrow$ pre) in the STDP curve, especially visible in panel F. Thus, the longer the inhibition lasts the more LTP we get at about $-50ms$. This is not a strong effect but it also shortens the time the synapse undergoes LTD. Note that the decay rate of the inhibitory neuron is mainly altered by a change in the calcium buffer parvalbumin (PV). In the pathological case PV is reduced and thus, we have a longer decay rate (see panels C,F) which in turn causes less LTD (see discussion section for more on this topic).

2.2. Realistic Model of STDP with Feedback Inhibition

So far we have been dealing with an abstract model which had the advantage that it could be treated analytically. With that model we have shown that feedback inhibition reduces the width of the LTD window. However, we have not been able to determine if the GAD67 or the NMDA hypofunction model is the most likely. In the theoretical model both hypothesis have lead to the same result because they just cause a linear gain change in the interneuron. We will show that a more realistic simulation will reveal a difference because changes in the NMDA receptor activation in the interneuron or an altered GABA production will lead to different effects in the feedback loop. While a reduction in NMDA receptor activity might change *spiking* behaviour in the interneuron, a change in GABA concentration will directly change the *amount* of inhibition acting on the pyramidal neuron. For that reason we investigate in a biophysically realistic model to which extent those hypotheses have an effect on the shape of the STDP curve.

We created a realistic microcircuit using a custom version of the GENESIS-sim 2.3 modelling tool (Bower and Beeman 1998 which can be downloaded from isg.elec.gla.ac.uk) which consists of a modelled cortical pyramidal cell and an attached GABAergic inhibitory interneuron. Using the GENESIS-sim modelling tool, we created a cortical pyramidal cell composed of two compartments (one for the soma and one for the axon). The axon is connected to an inhibitory fast spiking interneuron composed of a single compartment. The interneuron in turn then causes shunting inhibition on the pyramidal neuron (Aihara et al., 2007; O'Mann and Paulsen, 2006).

$$
\begin{aligned}
-C_m \frac{dV_m}{dt} &= I_{mem} + I_{syn} + I_{Ca} & (13) \\
I_{mem} &= g_{Na}(V_m - E_{Na}) + g_K(V_m - E_k) \\
&\quad + g_L(V_m - E_L) & (14) \\
&\quad + g_G(V_m - E_{Cl}) & (15) \\
I_{syn} &= g_A(V_m - E_A) + g_N(t, V_m) \cdot (V_m - E_N) & (16)
\end{aligned}
$$

where g_{Na} is the sodium conductance, g_K the potassium conductance and g_L the leakage conductance. I_{syn} is the current generated from the AMPA and NMDA synapses, E_A is the reverse potential of the AMPA synapse, E_N is the reverse potential of the NMDA synapse and $E_{Cl} = -65mV$ which is identical to the resting potential of the pyramidal cell. This term (15) is not present for the interneuron.

The GABA inhibitory synapse is modelled as a double alpha function:

$$
g_G(t) = A \cdot g_{Cl} \frac{e^{-t/\tau_{Cl_1}} - e^{-t/\tau_{Cl_2}}}{\tau_{Cl_1} - \tau_{Cl_2}} \tag{17}
$$

where A is a normalization constant chosen so that $g_G(t)$ reaches a maximum value of g_{Cl}. The rise time is $\tau_{Cl_1} = 10^{-9}$ and the decay time is $\tau_{Cl_2} = 10^{-3}$.

The post-synaptic **calcium concentration** [Ca] is established by a low-threshold calcium current I_{Ca} whose equation can be described as:

$$
I_{Ca}(V_m) = g_{Ca}m^2h(V_m - E_{Ca}) \tag{18}
$$

where $g_{Ca} = 1.75$ mS/cm^2 is the maximum conductance value of the calcium current, V_m the cell membrane potential, E_{Ca} the reversal potential, the activation variable $\dot{m} = -\frac{1}{\tau_m(V)}[m - m_\infty(V)]$, the inactivation variable $\dot{h} = -\frac{1}{\tau_h(V)}[h - h_\infty(V)]$, with $m_\infty(V) = \frac{1}{1+e^{-\frac{V+52}{7.4}}}$, $\tau_m(V) = 0.44 + \frac{0.15}{e^{\frac{V+27}{10}} + e^{-\frac{(V+102)}{15}}}$, $h_\infty(V) = \frac{1}{1+e^{\frac{V+80}{5}}}$ and $\tau_h(V) = 22.7 + \frac{0.27}{e^{\frac{V+48}{4}} + e^{-\frac{V+407}{50}}}$ for a temperature of 36°C.

The change in calcium concentration is calculated from a single-exponential model (Traub and Llinas, 1977; De Schutter and Bower, 1994) which is implemented in the GENESIS simulator:

$$
\begin{aligned}
dC/dt &= B \cdot I_{Ca} - C/\tau_{Ca} & (19) \\
[Ca] &= [Ca_B] + C & (20)
\end{aligned}
$$

with $\tau_{Ca} = 30$ms, $[Ca_B] = 2$mM/litre and $B = 10^{12}$ (see GENESIS documentation).

The **AMPA conductance** is calculated as an alpha function:

$$
g_{AMPA}(t) = \rho(t) \cdot g_A \cdot \frac{e^{\frac{-t}{\tau_{A1}}} - e^{\frac{-t}{\tau_{A2}}}}{\tau_{A1} - \tau_{A2}} \tag{21}
$$

with rise and decay times $\tau_{A1} = 2$ ms and $\tau_{A2} = 4$ ms. The AMPA receptor conductance is multiplied by the weight ρ which is controlled by our learning rule (see below). The weight represents the number of AMPA receptors inserted into the cell membrane.

The **NMDA conductance** is calculated using (Koch, 1998b):

$$
g_{NMDA}(t, V_m) = g_N \cdot \frac{e^{\frac{-t}{\tau_{N1}}} - e^{\frac{-t}{\tau_{N2}}}}{1 + \eta \cdot [Mg] \cdot e^{-\gamma V_m}} \tag{22}
$$

with rise and decay times $\tau_{N1} = 2$ ms, $\tau_{N2} = 100$ ms and maximum conductance g_N. The Magnesium-block parameters are: $\gamma = 0.06$/mV, $\eta = 0.33$/mM and the magnesium concentration is [Mg] = 2mM. This can directly be compared to Eq. 2 from the analytical section with the only difference that we have added the magnesium-block which is needed for a realistic model of the NMDA channel.

The **learning rule** is similar to the one used to derive the analytical solution Eq.8 with the difference that we use the derivative of the calcium concentration instead of the membrane potential itself (Saudargiene et al., 2004; Tamosiunaite et al., 2006). Weight change results from the correlation of the

change of the calcium concentration of the pyramidal cell with the activation of the NMDA receptor:

$$\frac{d\rho}{dt} = \mu \cdot g_{NMDA}(t) \cdot \frac{d}{dt}[Ca] \tag{23}$$

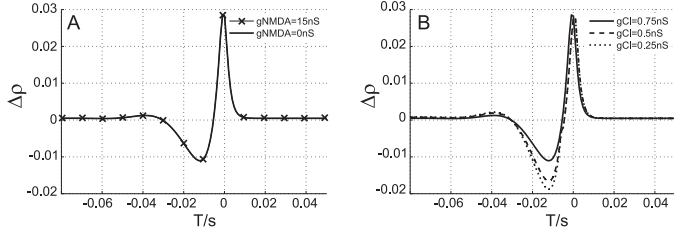where μ is the learning rate and $\frac{d\rho}{dt}$ is the change of AMPA receptors in the membrane.

Figure 3: Comparing the NMDA (A) with the GAD67 (B) hypothesis. A) Solid line: NMDA conductance of 15nS and dashed line with an NMDA conductance of 0 nS. Note, these curves are identical. B) STDP plot generated with different inhibition gains g_{Cl}. Solid line is $g_{Cl} = 0.75\ nS$, dashed line is $g_{Cl} = 0.5\ nS$, dotted line is $g_{Cl} = 0.25\ nS$. Parameters were for the pyramidal cell $g_{Na} = 65\ \mu S, g_K = 0.1\ \mu S, g_L = 25\ nS, E_{Na} = 0.055\ V, E_K = -0.090\ V, E_L = -0.065\ V, E_A = 0\ mV, E_N = 0\ mV$ and for the interneuron $g_{Na} = 65\ \mu S, g_K = 0.1\ \mu S, g_L = 25nS, E_{Na} = 0.055\ V, E_K = -0.090\ V, E_L = -0.065\ V, E_A = 0\ mV, E_N = 0\ mV$.

3. Results

As mentioned before the purpose of the realistic simulations is to determine which hypothesis should be favoured: the NMDA hypofunction or the GAD67 hypofunction. We tested the microcircuit (Fig. 1) with the same stimulation protocol we used in the analytical case: presynaptically we have one presynaptic action potential in form of a delta pulse which then activates both the NMDA and the AMPA receptors. At the postsynaptic input a current injection evokes a single action potential which in turn causes an action potential in the interneuron. The time T between pre- and postsynaptic current injection is defined as before.

3.1. NMDA hypofunction

We first tested the NMDA hypofunction hypothesis which states that reduced NMDA activation in the perisomatic interneurons will lead to less inhibition. This in turn should then lead to a wider LTD window. Consequently we changed the NMDA conductance g_N from its normal value $15nS$ to $0nS$. This can be seen in Fig. 3A. However, the STDP curves for both conditions $15nS$ and $0nS$ are identical where the latter actually means that we have no NMDA channels at all. What is the reason that the NMDA receptor has no influence on the shape of the STDP curve? The reasons behind it are the different reaction times of NMDA and AMPA receptors. The EPSPs of the NMDA channel always happens a bit later than the EPSP generated by the AMPA channel so that the interneuron is already spiking when the NMDA channel contributes to changes in the membrane potential. For that reason the NMDA receptor does not contribute to the spiking of the interneuron.
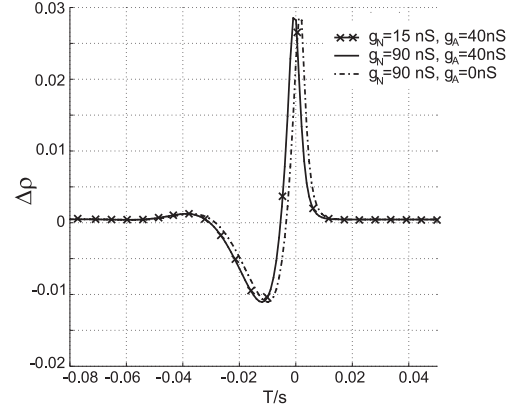

Figure 4: Further investigation of the role of the NMDA channel in STDP. Line with crosses: normal condition with $g_N = 15\ nS$ and $g_A = 40\ nS$. Solid line: stronger contribution of the NMDA channel with $g_N = 90\ nS$ and $g_A = 40\ nS$. Dashed line: NMDA channel generates the spike because the AMPA channel is switched off with $g_N = 90\ nS$ and $g_A = 0\ nS$.

In order to strengthen the point that the NMDA receptor in the interneuron has no contribution to the shape of the STDP curve we ran 3 simulations where we first increased the NMDA conductance and then switched off the AMPA channel (see Fig. 4). Note that for standard interneurons the maximum conductance of the NMDA receptor is about 10% of the AMPA receptor, meaning that the contribution to an EPSP is mainly through the AMPA receptor (Angulo et al., 1999). However, to investigate the influence of the NMDA receptor we increased its conductance from 15 nS to 90 nS making the NMDA receptor two times stronger than the AMPA receptor (see Fig. 4 solid line). However, the increase in NMDA conductance does not change the shape of the STDP curve compared to the control condition (line with crosses). This confirms what has been said in the previous paragraph: the NMDA receptor is too slow so that the AMPA receptor has already caused the interneuron to spike. Finally, to investigate the contribution of the NMDA receptor itself to the STDP curve we switched off the AMPA receptor completely (dashed line) and leave the NMDA conductance at 90 nS because at 15 nS the interneuron would not spike. In this case we get the same STDP curve but shifted about 1ms to the right. This is expected because it is the slower reaction time of the NMDA receptor which causes the interneuron to spike slightly later. However, at this point we have created a very unrealistic situation to see an effect at all: the NMDA conductance is six times higher than normal and there is no AMPA channel. Coming back to normal AMPA and NMDA conductances makes it clear that spikes in interneurons are caused by AMPA channels and not by NMDA channels. In conclusion it seems so that reduced NMDA receptor activation will not lead to a change in the STDP curve because the contribution of the NMDA receptor is too small and it reacts too slow against the AMPA receptor.

Finally, we also tested the overall robustness of the model. The STDP shape is robust to variation of the NMDA and AMPA conductances on both the interneuron and the pyrami-

dal cell. This is mainly due to the fact that we have spiking neurons because as long as they generate the same amount of spikes the results will be very similar. Even this requirement can be relaxed for the interneuron which is allowed to spike one or two times without changing the results as long as the conductances are $g_N \epsilon [15nS \dots 49nS]$, $g_A \epsilon [45nS \dots 68nS]$ and $g_{Cl} \epsilon [0.01nS \dots 10.0nS]$. The pyramidal neuron needs to spike once so that we have a properly defined spike timing which is the case when $g_N \epsilon [15nS \dots 90nS]$, $g_A \epsilon [0nS \dots 40nS]$ and $g_{Cl} \epsilon [0.01nS \dots 10.0nS]$. As mentioned above the other necessary condition is that the NMDA decay time is longer than the AMPA decay time $\tau_{N2} > \tau_{A2}$ which is always the case in biophysically realistic cases.
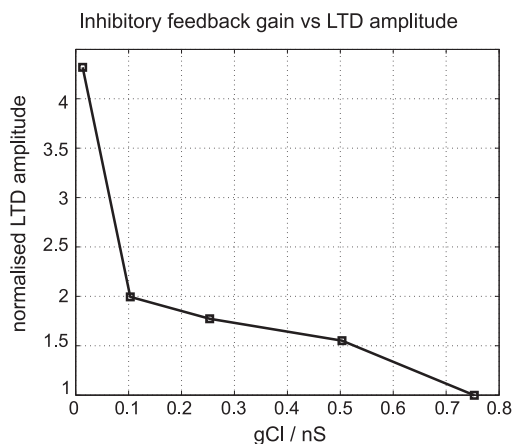

Figure 5: Relation between the GABA inhibition and the LTD amplitude: plot of the normalised LTD amplitudes against the g_{Cl} conductance of the GABA receptor on the pyramidal neuron. Normalisation against the LTD amplitude at $g_{Cl} = 0.75\,nS$.

3.2. GAD67 hypofunction

The second group of simulations were done by reducing the conductance of the GABA synapse, simulating a reduction of the GABA release due to a hypofunction of GAD67. We determined the STDP curve using inhibitions of different strengths (see Fig. 3B) by changing the Cl conductance from 0.75 nS to 0.25 nS. With strong inhibition we have the same STDP curve as in Fig. 3A that was generated for $g_{Cl} = 0.75\,nS$. With less strong inhibition the depth of LTD increases from -0.01 to -0.02 while the LTP part is unaffected. Thus, a reduction of GABA to a third of its original value leads to a change of the LTD part of the STDP curve.

In contrast to the NMDA hypothesis the GAD67 hypothesis is a rather gradual phenomenon because the GABA release can be gradually reduced which can already be seen in Fig. 3B: the more inhibitory gain the less LTD. To demonstrate this more clearly we have plotted in Fig. 5 the relation between the inhibitory gain g_{Cl} and the amplitude of the LTD part of the STDP curve. The conductance $g_{Cl} = 0.75nS$ is our reference point as it is the conductance under normal conditions. If we decrease the conductance, the LTD amplitude increases gradually to about two times the original level at $g_{Cl} = 0.1nS$ and then

increases to over four times the original amplitude. The shape of the curve is approximately that of an $f(x) = 1/x$ function which is expected for shunting inhibition.

In conclusion we see that the STDP curve will change rather gradually with altered GABAergic inhibition. This also means that even small changes in the GABA release will actually cause changes of the shape of the STDP curve because it is a linear process.

3.3. GAD67 hypothesis is more likely than NMDA hypofunction

Comparing the results it is apparent that a reduced GAD67 hypofunction is most likely the cause for cortical hypofunction rather than the NMDA hypofunction. This is because the NMDA receptors contribute poorly to the EPSP in the interneuron in contrast to the much stronger AMPA receptors. On the contrary the GAD67 defect reduces the GABA release gradually and will always lead to a reduction in inhibition. In other words: small changes in GAD67 will lead to small changes in the STDP curve and vice versa. For that reason the GAD67 hypothesis seems to be more probable.

4. Discussion

We have shown that a *reduction* of inhibitory function in cortical micro-circuits *increases* the contribution of LTD in spike timing dependent plasticity. We tested the so called NMDA hypothesis and the GAD67 hypothesis to find out which one is the most likely candidate to cause more synaptic depression. The results from our realistic simulations point clearly towards the GAD67 hypothesis.

The predicted sustained long term depression in the cortex will also lead in the long run to the pruning of the affected synapses (Shinoda et al., 2005). The link between synaptic pruning and Schizophrenia has been investigated for nearly 3 decades (Feinberg, 1982; Rapoport et al., 2005; Iglesias and Villa, 2007) and is well established. Consequently, the results of our study suggest that the synapses which have undergone LTD for a sustained time will be pruned and will no longer be part of the cortical network.

In this paper we have focussed on the loss of inhibitory function. Other argue that there is some evidence that the number of PV cells is reduced (Beasley and Reynolds, 1997) and also that the number of axon terminals on the axon initial segment is reduced (Pierri et al., 1999). However, the general consensus tends towards a *loss of function*, reflected in PV and GAD67 expression (Straub et al., 2007; Guidotti et al., 2005), a reduced NMDA mediated input as well as a reduced inhibitory output (Kehrer et al., 2008).

Virtually all modern hypotheses about Schizophrenia focus on the hypofunction of inhibitory neurons in the prefrontal cortex (Paz et al., 2008; Lisman et al., 2008; Lewis et al., 2005). However there are conflicting views on which defect in the inhibitory neurons is responsible for its hypofunction. Two major hypothesis have been brought forward: one centres around NMDA hypofunction and the other around a reduction

of GAD67 where the latter is an enzyme responsible for the synthesis of GABA. We are first discussing the GAD67 hypothesis and then the NMDA hypothesis.

GAD67 is an enzyme that synthesises GABA in the inhibitory neurons (Straub et al., 2007; Guidotti et al., 2005). Indeed a strong reduction of GAD67 is found in the prefrontal cortex of Schizophrenic patients (Akbarian et al., 1995). GAD67 in turn is driven by TrkB which is also reduced in Schizophrenic patients and is a strong candidate for the actual cause of Schizophrenia (Lewis et al., 2005). A reduction of GAD67 works on the release side and is therefore graded. In the GAD67 model a reduction of GABA release could be virtually any fraction compared to control whereas NMDA hypofunction can only change the number of spikes after an EPSP in the inhibitory neuron. The less GAD67 is synthesised in the interneuron the less GABA will be released which causes a rather gradual reduction in inhibition. This model is straightforward and can easily explain the cortical hypofrontality in Schizophrenia and has a direct effect on the STDP curve.

In contrast to the GAD67 hypothesis the NMDA hypothesis is rather inconsistent. The model for NMDA hypofunction gains its momentum from the effects which NMDA antagonists have on cortical and cognitive function, especially Ketamine and PCP (Morris et al., 2005). Administered in humans, they cause *instantly* hallucinations and other symptoms known from Schizophrenic patients. In rodents after *chronic* application they impair extra-dimensional set shift tasks which are associated with prefrontal cortical dysfunction (Egerton et al., 2008). Note the difference in the experimental setup: while in humans the deficits show up instantly after application of PCP or Ketamine, in the animal model they appear only after chronic application of 5 days or more.

The observed effects point to a rather complex interaction of different factors compared to the straightforward interpretation of the GAD67 hypothesis. From our simulations above we have learned that a reduced NMDA receptor activity will not lead to a change in STDP. From that it is clear that STDP seems not to be the cause for the long term effects after chronic administration. We need to look closer into the effects of the NMDA antagonists.

An interesting aspect of the NMDA hypothesis arises from the fact that this is an input related defect: NMDA hypofunction needs to be detrimental enough to prevent spiking in the interneuron or at least is able to reduce the number of spikes. This can only work if the NMDA receptors have a strong contribution to the EPSP in interneurons. However, even a "strong" contribution of the NMDA receptor to the EPSP seems to be only in the range of a few percent (Angulo et al., 1999) which weakens the point that NMDA hypofunction has a strong influence on the spiking behaviour of interneurons.

So far we have been discussing only a change of the gain of the inhibition and not the timing of the inhibition. Neurons which have reduced NMDA functioning contain the Calcium buffer parvalbumin (PV). This buffer modulates especially the decay of the Calcium concentration after a spike. There is evidence that in Schizophrenic patients the parvalbumin concentration in the interneurons is reduced. This leads to a longer

time constant of the calcium decay after a spike in the interneuron. It has been proposed that the reduction of PV in Schizophrenia is a compensatory mechanism which aims to increase the gain of the interneurons and therefore the inhibition (Lisman et al., 2008). However, we have shown in the GENESIS model that the longer inhibition by the Ca dynamics has no influence on the STDP curve.

On the network level this looks a bit different because a diminished NMDA activation will have an effect because of less longer lasting inhibition. This means that on the network level less NMDA activation will lead to more activity. This has been recently pointed out by Lisman et al. (2008) who proposes that cells in fact reduce their PV concentration to "fake" the longer NMDA activation in interneurons. While this has no effect on the STDP curve this is an important property for network stability which leads to the last point, namely network effects.

This study has dealt with feedback inhibition and how it influences spike-timing dependent plasticity. While mainly basket cells are responsible for feedback inhibition, Chandelier cells are mainly responsible for feedforward inhibition. However, Chandelier cells do not innervate the cell body but the initial axon segments of the pyramidal neurons ("cartridges") and have therefore little influence on the somatic potential which in turn is responsible for the shape of the STPD curve. A hypofunction of the chandelier cells has strong effects on the wider cortical network, especially working memory. In these wider networks oscillations in the gamma frequency range are important to guarantee proper processing. This goes far beyond this paper as it requires a working memory model and will be investigated in the future.

The classical model of spike-timing dependent plasticity measures the time between pre- and post-synaptic potentials and then looks up the weight change in a predefined function. Generally this is either created specifically, or is derived from rather computational principles, for example, the "spike response" model (Jolivet et al., 2003). Recently, this classical model has been improved by taking into account the postsynaptic potential (Clopath et al., 2010). In our case the STDP curve emerges by integrating the learning rule (Eq. 8) which is based on biophysical parameters. The advantage of this is that we are not limited to two discrete time events (e.g. pre- and postsynaptic spike) but can actually calculate STDP in a network with many inputs without complicating the model and/or increasing the computational complexity (Tamosiunaite et al., 2006). This is especially important in our model where we have three events occurring; the pre-synaptic input, the postsynaptic input and then the third being the inhibitory feedback from the interneuron. This model could also be extended to include more complex dendritic input dynamics which arise when we take into account backpropagating spikes and local calcium spikes in distal dendrites as investigated in Tamosiunaite et al. (2007a,b). However, this would go far beyond the scope of this paper and would prevent an analytical treatmeant so that we have concentrated here on short range connectivity close to the soma which can be assumed to happen simultaneously.

The learning rule (Eq. 23) uses the derivative of the calcium concentration (Eq. 19) which in turn has been modelled as a first

order low-pass which lumps together the biophysical parameters of the calcium dynamics (De Schutter and Bower, 1994) caused by the influx of calcium through the NMDA channel (De Schutter and Bower, 1993). Our phenomenological model about the calcium dynamics could be enhanced by a more detailed calcium model as outlined in Rubin et al. (2005) which takes into account the complex interactions between the calcium channels and the calcium concentration. However, this would make a direct comparison between the analytical and biophysically realistic model more difficult.

Possible ways of treatment are consequently the boosting of the inhibitory system. Our plasticity model predicts that those drugs should be successful which increase the "gain" of the inhibitory system. For example, benzodiazepines increase the gain of the GABA transmission by increasing the frequency of the Cl channels. On the other hand, we predict that GABA agonists will not be suitable to boost LTP in the cortical circuitry because they just increase the inhibitory bias on the pyramidal neurons but not the *change* of the postsynaptic potential which is ultimately responsible for the shape of the STDP curve.

Acknowledgements

References

Aihara, T., Y. Abiru, Y. Y., H. Watanabe, Y. F., Tsukada, M., 2007. The relation between spike-timing dependent plasticity and Ca^{2+} dynamics in the hippocampal CA1 network. Neuroscience 145, 80–87.

Akbarian, S., Kim, J. J., Potkin, S. G., Hagman, J. O., Tafazzoli, A., Bunney, W. E., Jones, E. G., Apr 1995. Gene expression for glutamic acid decarboxylase is reduced without loss of neurons in prefrontal cortex of schizophrenics. Arch Gen Psychiatry 52 (4), 258–266.

Andreasen, N. C., O'Leary, D. S., Flaum, M., Nopoulos, P., Watkins, G. L., Boles Ponto, L. L., Hichwa, R. D., Jun 1997. Hypofrontality in schizophrenia: distributed dysfunctional circuits in neuroleptic-naïve patients. Lancet 349 (9067), 1730–1734.

Angulo, M. C., Rossier, J., Audinat, E., Sep 1999. Postsynaptic glutamate receptors and integrative properties of fast-spiking interneurons in the rat neocortex. J Neurophysiol 82 (3), 1295–1302.

Beasley, C. L., Reynolds, G. P., Apr 1997. Parvalbumin-immunoreactive neurons are reduced in the prefrontal cortex of schizophrenics. Schizophr Res 24 (3), 349–355.
URL http://www.hubmed.org/display.cgi?uids=9134596

Bi, G.-q., Poo, M.-m., 1998. Synaptic modifications in cultured hippocampal neurons: Dependence on spike timing, synaptic strengh, and postsynaptic cell type. J Neurosci 18 (24), 10464–10472.

Bower, J., Beeman, D., 1998. The Book of GENESIS: Exploring Realistic Neural Models with the GEneral NEural SImulation System (2nd Ed.). Springer-Verlag, New York.

Clopath, C., Büsing, L., Vasilaki, E., Gerstner, W., 2010. Connectivity reflects coding: A model of voltage-based spike-timing-dependent-plasticity with homeostasis. Nature Neuroscience 13, 344–352.

De Schutter, E., Bower, J., 1993. Sensitivity of synaptic plasticity to the ca2+ permeability of nmda channels: a model of long-term potentiation in hippocampal neurons. Neural Computation 5, 681–694.

De Schutter, E., Bower, J. M., Jan 1994. An active membrane model of the cerebellar purkinje cell. i. simulation of current clamps in slice. J Neurophysiol 71 (1), 375–400.
URL http://www.hubmed.org/display.cgi?uids=7512629

Egerton, A., Reid, L., McGregor, S., Cochran, S. M., Morris, B. J., Pratt, J. A., May 2008. Subchronic and chronic pcp treatment produces temporally distinct deficits in attentional set shifting and prepulse inhibition in rats. Psychopharmacology (Berl) 198 (1), 37–49.

Feinberg, I., 1982. Schizophrenia: caused by a fault in programmed synaptic elimination during adolescence? J Psychiatr Res 17 (4), 319–334.
URL http://www.hubmed.org/display.cgi?uids=7187776

Freund, T. F., Katona, I., Oct 2007. Perisomatic inhibition. Neuron 56 (1), 33–42.
URL http://www.hubmed.org/display.cgi?uids=17920013

Guidotti, A., Auta, J., Davis, J. M., Dong, E., Grayson, D. R., Veldic, M., Zhang, X., Costa, E., Jul 2005. Gabaergic dysfunction in schizophrenia: new treatment strategies on the horizon. Psychopharmacology (Berl) 180 (2), 191–205.

Hebb, D. O., 1949. The organization of behavior: A neuropyschological theory. Wiley-Interscience, New York.

Iglesias, J., Villa, A. E., May-Jun 2007. Effect of stimulus-driven pruning on the detection of spatiotemporal patterns of activity in large neural networks. Biosystems 89 (1-3), 287–293.
URL http://www.hubmed.org/display.cgi?uids=17324499

Jolivet, R., Lewis, T., Gerstner, W., 2003. The Spike Response Model: A framework to predict neuronal spike trains. In: et al., K. (Ed.), Proc. Joint International Conference ICANN/ICONIP 2003.

Kehrer, C., Maziashvili, N., Dugladze, T., Gloveli, T., 2008. Altered excitatory-inhibitory balance in the nmda-hypofunction model of schizophrenia. Front Mol Neurosci 1, 6–6.

Klopf, A. H., 1986. A drive-reinforcement model of single neuron function. In: Denker, J. S. (Ed.), Neural Networks for Computing: Snowbird, Utah. Vol. 151 of AIP conference proceedings. American Institute of Physics, New York.

Koch, C., 1998a. Biophysics of Computation: Information Processing in Single Neurons. Oxford Uni. Press, New York.

Koch, C., 1998b. Biophysics of Computation: Information Processing in Single Neurons. Oxford University Press, New York USA.

Lewis, D. A., Hashimoto, T., Volk, D. W., Apr 2005. Cortical inhibitory neurons and schizophrenia. Nat Rev Neurosci 6 (4), 312–324.

Lindskog, M., Kim, M. S., Wikstrom, M., Blackwell, K. T., Kotaleski, J. H., 2006. Transient calcium and dopamine increase PKA activity and DARPP-32 phosphorylation. PLoS Comput Biol 2, 1045–1060.

Lisman, J. E., Coyle, J. T., Green, R. W., Javitt, D. C., Benes, F. M., Heckers, S., Grace, A. A., May 2008. Circuit-based framework for understanding neurotransmitter and risk gene interactions in schizophrenia. Trends Neurosci 31 (5), 234–242.

Magee, J. C., Johnston, D., 1997. A synaptically controlled, associative signal for Hebbian plasticity in hippocampal neurons. Science 275, 209–213.

Markram, H., Lübke, J., Frotscher, M., Sakman, B., 1997. Regulation of synaptic efficacy by coincidence of postsynaptic APs and EPSPs. Science 275, 213–215.

Morris, B. J., Cochran, S. M., Pratt, J. A., 2005. PCP: from pharmacology to modelling schizophrenia. Curr opinion Pharmacology 5.

O'Mann, E., Paulsen, O., 2006. Keeping Inhibition Timely. Neuron 49 (1), 8–9.

Paz, R. D., Tardito, S., Atzori, M., Tseng, K. Y., Nov 2008. Glutamatergic dysfunction in schizophrenia: from basic neuroscience to clinical psychopharmacology. Eur Neuropsychopharmacol 18 (11), 773–786.

Pierri, J. N., Chaudry, A. S., Woo, T. U., Lewis, D. A., Nov 1999. Alterations in chandelier neuron axon terminals in the prefrontal cortex of schizophrenic subjects. Am J Psychiatry 156 (11), 1709–1719.
URL http://www.hubmed.org/display.cgi?uids=10553733

Porr, B., Saudargiene, A., Wörgötter, F., 2004. Analytical solution of spike-timing dependent plasticity based on synaptic biophysics. In: Thrun, S., Saul, L., Schölkopf, B. (Eds.), Advances in Neural Information Processing Systems 16. MIT Press, Cambridge, MA.

Porr, B., Wörgötter, F., 2003. Isotropic Sequence Order learning. Neural Comp. 15, 831–864.

Ragland, J. D., Yoon, J., Minzenberg, M. J., Carter, C. S., Aug 2007. Neuroimaging of cognitive disability in schizophrenia: search for a pathophysiological mechanism. Int Rev Psychiatry 19 (4), 417–427.

Rapoport, J. L., Addington, A. M., Frangou, S., Psych, M. R., May 2005. The neurodevelopmental model of schizophrenia: update 2005. Mol Psychiatry 10 (5), 434–449.
URL http://www.hubmed.org/display.cgi?uids=15700048

Rubin, J. E., Gerkin, R. C., Bi, G. Q., Chow, C. C., May 2005. Calcium time course as a signal for spike-timing-dependent plasticity. J Neurophysiol 93 (5), 2600–2613.
URL http://www.hubmed.org/display.cgi?uids=15625097

Saudargiene, A., Porr, B., Wörgötter, F., 2004. How the shape of pre- and post-synaptic signals can influence stdp: A biophysical model. Neural Comp. 16, 595–626.

Shinoda, Y., Kamikubo, Y., Egashira, Y., Tominaga-Yoshino, K., Ogura, A., Apr 2005. Repetition of mglur-dependent ltd causes slowly developing persistent reduction in synaptic strength accompanied by synapse elimination. Brain Res 1042 (1), 99–107.
URL http://www.hubmed.org/display.cgi?uids=15823258

Somogyi, P., Klausberger, T., Jan 2005. Defined types of cortical interneurone structure space and spike timing in the hippocampus. J Physiol 562 (Pt 1), 9–26.

Straub, R. E., Lipska, B. K., Egan, M. F., Goldberg, T. E., Callicott, J. H., Mayhew, M. B., Vakkalanka, R. K., Kolachana, B. S., Kleinman, J. E., Weinberger, D. R., Sep 2007. Allelic variation in gad1 (gad67) is associated with schizophrenia and influences cortical function and gene expression. Mol Psychiatry 12 (9), 854–869.

Tamosiunaite, M., Porr, B., Wörgötter, F., 2006. Temporally changing synaptic plasticity. Advances in Neural Information Processing Systems 18. MIT Press, Cambridge, MA.

Tamosiunaite, M., Porr, B., Wörgötter, F., 2007a. Developing velocity sensitivity in a model neuron by local synaptic plasticity. Biological Cybernetics 96 (5), 507–518.

Tamosiunaite, M., Porr, B., Wörgötter, F., Aug 2007b. Self-influencing synaptic plasticity: recurrent changes of synaptic weights can lead to specific functional properties. J Comput Neurosci 23 (1), 113–127.

Traub, R., Llinas, R., 1977. The spatial distribution of ionic conductances in normal and axotomized motoneurons. Neuroscience 2, 829–850.

Ulrich, D., Oct 2003. Differential arithmetic of shunting inhibition for voltage and spike rate in neocortical pyramidal cells. Eur J Neurosci 18 (8), 2159–2165.

Voegtlin, T., 2009. Adaptive synchronization of activities in a recurrent network. Neural Computation 21 (6), 1749–1775.

Yang, S. N., Tang, Y. G., Zucker, R. S., Feb 1999. Selective induction of LTP and LTD by postsynaptic [Ca2+]i elevation. J Neurophysiol 81 (2), 781–787.

Zaitsev, A. V., Povysheva, N., Lewis, D. A., Krimer, L. S., 2007. P/Q-Type, But Not N-Type, Calcium Channels Mediate GABA Release From Fast-Spiking Interneurons to Pyramidal Cells in Rat Prefrontal Cortex. J Neurophysiol 97, 3567–3573.